Published in final edited form as:
Eur J Neurol. 2012 March ; 19(3): 488–493. doi:10.1111/j.1468-1331.2011.03570.x.

Glucose metabolism in sporadic Creutzfeldt-Jakob disease: an SPM Analysis of ^{18}F-FDG PET

Eun-Joo Kim, M.D.[1], **Sang-Soo Cho, Ph.D.**[2], **Byung-Hoon Jeong, Ph.D.**[3], **Yong-Sun Kim, M.D.**[3], **Sang Won Seo, M.D.**[4], **Duk L. Na, M.D.**[4], **Michael D. Geschwind, M.D., Ph.D.**[5], and **Yong Jeong, M.D., Ph.D.**[4,6]

[1]Department of Neurology, Pusan National University Hospital, Pusan National University School of Medicine and Medical Research Institute, Busan, Korea

[2]PET Imaging Center, Centre for Addiction and Mental Health, University of Toronto, Toronto, Canada

[3]Ilsong Institute of Life Science, Hayllym University, Anyang, Korea

[4]Department of Neurology, Samsung Medical Center, Sungkyunkwan University School of Medicine, Seoul, Korea

[5]Memory and Aging Center, Department of Neurology, University of California, San Francisco, San Francisco, California, USA

[6]Department of Bio and Brain Engineering, KAIST, Daejeon, Korea

Abstract

Background and purpose—Reports describing functional neuroimaging techniques, such as positron emission tomography (PET) and single photon emission computed tomography (SPECT), in sporadic Creutzfeldt-Jakob disease (sCJD) have consistently suggested that these tools are sensitive for the identification of areas of hypoperfusion or hypometabolism, even in the early stages of sCJD. However, there are few reports on the use of [18F]fluoro-2-deoxy-D-glucose (FDG) PETin sCJD and most of them are single case reports. Only two small cohort studies based on visual inspection or a region of interest method have been published to date. Using a statistical parametric mapping (SPM) analysis of ^{18}F-FDG PET, we investigated whether there are brain regions preferentially affected in sCJD.

Methods—After controlling for age and gender, using SPM 2 we compared the glucose metabolism between i) 11 patients with sCJD and 35 controls and ii) the subset of 5 patients with the Heidenhain variant of sCJD and 35 controls.

Results—The patients with sCJD showed decreased glucose metabolism in bilateral parietal, frontal, and occipital cortices. The Heidenhain variant of sCJD showed glucose hypometabolism mainly in bilateral occipital areas.

Conclusions—Glucose hypometabolism in sCJD was detected in extensive cortical regions; however, it was not found in the basal ganglia or thalamus, which are frequently reported to be affected on diffusion-weighted images. The medial temporal area, which is possibly resistant to the prion deposits, was also less involved in sCJD.

Corresponding author: Yong Jeong, M.D., Ph.D., Department of Bio and Brain Engineering, KAIST, 291 Daehak-ro, Yuseong-gu, Daejeon 305-701, Korea, Tel: +82-42-350-4324, Fax: +82-42-350-4310, yong@kaist.ac.kr.

Competing Interest: None declared.

Financial Disclosures : None relevant reported.

NIH-PA Author Manuscript

NIH-PA Author Manuscript

Keywords

Creutzfeldt-Jakob disease; prion disease; PET

Introduction

Creutzfeldt-Jakob disease (CJD) is characterized by rapidly progressive dementia with a variety of neurological symptoms and a fatal outcome. Structural neuroimaging, such as MRI, is an important diagnostic tool for sporadic CJD (sCJD). High signal changes in the cerebral cortex, basal ganglia, or thalamus on fluid-attenuated inversion recovery (FLAIR) and diffusion-weighted images (DWIs), in particular, have high sensitivity and specificity for sCJD even in the early stage of the disease [1–5]. However, although there are a few publications on the use of functional neuroimaging in sCJD, most [18F]fluoro-2-deoxy-D-glucose (FDG) positron emission tomography (PET) publications are single case reports and few small cohort studies of ^{18}F-FDG-PET in sCJD relied on visual inspection or a region of interest (ROI) method [6–17]. Although the ROI technique is a useful method, it can only analyze selected areas, and therefore remaining brain regions may be left unexplored. To date, we are not aware of any study that has used statistical parametric mapping (SPM) analysis to compare the glucose metabolism of patients with sCJD to that of normal controls. Thus, the aims of this study were to use SPM analysis of FDG-PET in sCJD patients to examine (i) which brain regions are preferentially affected in sCJD and (ii) if there are any different hypometabolic patterns associated with Heidenhain variant of sCJD.

Methods

Subjects

Among 28 consecutive patients with sCJD seen from March 1, 1998 to December 31, 2005 at the Department of Neurology, Samsung Medical Center, 13 who had received ^{18}F-FDG-PET scans were initially selected. After excluding 2 patients whose ^{18}F- FDG PETs were imaged with a different scanner, 11 (5 male, 6 female; mean age 61.6 ± 10.0 years; range 36–75 years) were enrolled in this study. Using the World Health Organization (WHO) 1998 diagnostic criteria for sCJD, one patient was a definite, seven were probable, and three were possible cases [18]; all cases met UCSF 2007 probable sCJD criteria based on their symptoms and positive DWI brain MRI (Table 1) [19]. All 11 patients underwent brain MRI 1.7 ± 2.3 days before undergoing PET scans, and the average time interval from symptom onset to PET or MRI was 2.9 ± 2.3 months. Except one patient who could not be traced, total disease duration of 10 out 11 patients was an average of 10.6 ± 11.6 months. Five patients with visual disturbance as the first symptom (2 male, 3 female; mean age 58.0 ± 13.5 years; range 36–69 years) were classified as the Heidenhain variant of CJD [20]. The clinical features of the patients and the regions with high signal intensities on DWIs are summarized in Table 1. All five patients who underwent genotyping of the prion protein gene (PRNP) (2 male, 3 female; mean age 59.0 ± 14.0 years; range 36–75 years) demonstrated methionine homozygosity (MM) at codon 129. None of patients in this study had a family history of CJD.

The control group consisted of 35 healthy volunteers (18 male, 17 female; mean age 62.5±8.2 years; range 49–74 years) who had neither a history of neurological and psychiatric illness nor abnormalities on neurological examinations. The Samsung Medical Center Institutional Review Board and an ethical standards committee approved this study.

PET imaging and image analysis

PET scans of 30 min were acquired starting 40 min after intravenous injection of 4.8 MBq/kg FDG using a GE Advance PET scanner. In-plane and axial resolution of the scanner was 4.9 and 3.9 mm full-width at half maximum, respectively. Subjects fasted for at least 4 h before PET scanning. PET images were reconstructed using a Hanning filter (cut-off frequency = 4.5 mm) and displayed in 128 × 128 matrix (pixel size = 1.95 × 1.95 mm with a slice thickness of 4.25 mm). Attenuation correction was performed with a uniform attenuation coefficient ($\mu = 0.096\ cm^{-1}$).

PET images were analyzed using SPM 2 (Wellcome Department of Cognitive Neurology, Institute of Neurology, London, UK). Prior to statistical analysis, all the images were spatially normalized into the MNI standard template (Montreal Neurological Institute, McGill University, Montreal, Canada) to remove inter-subject anatomical variability. Spatially normalized images were smoothed by convolution, using an isotropic Gaussian kernel with 12-mm FWHM. The count of each voxel was normalized by proportional scaling to the average whole brain activity and fit to a linear statistical model by the method of least squares. Statistical comparisons between groups were performed on a voxel-by-voxel basis using *t* statistics, generating SPM (*t*) maps. We investigated hypometabolic brain areas at a height threshold of $P = 0.05$ (corrected) and an extent threshold of 100 voxels. For visualization of the t-score statistics (SPM{t, #1} map), the significant voxels were projected onto the 3D rendered brain or a standard high-resolution MRI template thus allowing anatomic identification. We made the following comparisons using age and gender as covariates: (1) Total sCJD versus controls and (2) the Heidenhain variant of sCJD versus controls.

Results

Compared to controls, patients with sCJD showed decreased glucose metabolism in bilateral parietal, frontal, and occipital cortices and middle and superior temporal gyri with a right-sided predominance ($p < 0.05$, corrected for multiple comparisons, $k = 100$, Fig. A). Patients with the Heidenhain variant of sCJD showed glucose hypometabolism mainly in bilateral occipital and parietal areas with a right-sided predominance ($p < 0.05$, corrected for multiple comparisons, $k = 100$, Fig. B). The right middle frontal and superior temporal gyri were also detected as hypometabolic regions.

Discussion

In our study, patients with sCJD showed glucose hypometabolism in extensive cortical regions, including bilateral frontal, parietal, and occipital areas, compared with normal controls. This finding is consistent with DWI studies in sCJD [1–5]. One of the most interesting finding was that the basal ganglia as well as the thalamus, two areas commonly involved in sCJD (particularly the basal ganglia) in MRI studies [1, 2, 4, 5], were unaffected in the context of metabolism. This result is compatible with a previous ^{18}F-FDG PET group study based on a ROIs method that found the putamen and thalamus were less affected in 9 patients [16] and with most case reports, which did not show involvement of deep gray matter [6–9, 11–14]. Another PET study showed that only 1 out of total 8 patients with sCJD demonstrated involvement of the cerebellum, which is also be compatible with our results [15].

All the patients underwent brain MRIs and ^{18}F-FDG PET scans on almost the same day, and 9 out of 11 patients with sCJD demonstrated increased signal intensities of the basal ganglia on DWI sequences. Even though the cause of high signal changes on DWI in sCJD remains unclear, several studies have reported that these MR changes correlate with certain neuropathological findings, particularly vacuolation and prion (PrP^{Sc}) accumulation, regardless of cortical and subcortical lesions [21–24]. Therefore, the reason why the basal ganglia, which was detected as having high signal intensities on DWI that were similar to other cortical regions, did not demonstrate hypometabolism on ^{18}F-FDG PET remains unclear. One possibility is that vacuolation and/or prion deposition do not always correlate with neuronal dysfunction and hypometabolism. Furthermore, as MRI abnormalities in most sCJD cases appear first cortically and then move subcortically over time, this suggests that the cortex is affected earlier and thus longer than subcortical structures. The deep nuclei in this cohort thus might be less affected physiologically at the times of the FDG-PET scans. It is possible that if patients were followed longitudinally to later stages of disease that subcortical involvement would be evident on FDG-PET imaging.

Another interesting finding of our study was that patients with sCJD did not show hypometabolism in the medial temporal area e.g. hippocampus and amygdala, which is also consistent with a previous PET study showing the temporal area was relatively less affected in sCJD [16] and with a pathological study suggesting possible resistance of hippocampus to the prion deposits in CJD [25, 26].

In our study, the glucose hypometabolism of patients with the Heidenhain variant was found mainly in the parietooccipital areas, which agreed with the results of the previous studies [7, 10–13]. This finding may explain the clinical symptoms of patients with the variant.

To our knowledge, there have been few published studies on PET findings according to the molecular subtypes of sCJD [27]. Although we did not have prion typing data, all five patients tested for codon 129 polymorphism were MM and we suspect that most were MM given its prevalence in the Korean sCJD population [28]. A recent MRI study of a large number of patients with sCJD described that the basal ganglia, frontal lobes, parietal lobes, and cingulate gyri were frequently affected in the MM1 subtype, while the thalamus, cerebellum, and temporal lobes were frequently involved in the MM2 subtype [29]. Regarding the asymmetric involvement with right-sided predominance in our study (Fig. A), there have been several reports regarding asymmetric cortical involvement in sCJD, but the results were inconsistent [30–34]. One recent DWI MRI study of 49 sCJD subjects suggests the possibility of left-sided involvement to be more common [1].

Although MR DWI is the most sensitive imaging tool for the clinical diagnosis of CJD, functional imaging remains a useful technique that supports DWI findings [11, 15, 16, 35]. It is interesting to see if ^{18}F-FDG PET has diagnostic utility in CJD, however, rare group studies using ^{18}F-FDG PET in CJD have been reported.

Our study has limitations including a small sample size and lack of pathological confirmation of most diagnoses. Also, because the patients in this study had had an average disease duration of 10.6 ± 11.6 months with FDG-PET scans performed at an average of 2.9 ± 2.3 months after onset of clinical symptoms and no patients had follow-up FDG-PET scans, we could not exclude the possibility if the subjects had longer duration of symptoms prior to FDG-PET scans, they might have had demonstrated further neuronal damage extend to basal ganglia or thalamus on FDG-PET. Despite of these limitations, we think that our findings provide useful information regarding the functional neuroimaging findings of sCJD and that these findings will be confirmed in future studies with larger, pathology-confirmed series. The lack of deep nuclei hypometabolism on ^{18}F-FDG PET despite DWI involvement needs to be explored further. Although this study did not assess whether FDG-PET is helpful for diagnosis, in some cases even might reveal abnormalities earlier than MRI [36] and at a minimum might improve our understanding of the physiological processes underlying sCJD.

Acknowledgments

This research was supported by World Class University program through the National Research Foundation of Korea funded by the Ministry of Education, Science and Technology (R32-2008-000-10218-0) to YJ, a grant of the Korea Healthcare technology R&D Project, Ministry of Health and Welfare, Republic of Korea (A102065) and Medical Research Institute Grant (2009–11), Pusan National University Hospital to EJK, and US NIH/NIA R01 and the Michael J. Homer Family fund to MDG.

References

1. Vitali P, Maccagnano E, Caverzasi E, et al. Diffusion-weighted MRI hyperintensity patterns differentiate CJD from other rapid dementias. Neurology. 2011; 76:1711–1719. [PubMed: 21471469]
2. Shiga Y, Miyazawa K, Sato S, et al. Diffusion-weighted MRI abnormalities as an early diagnostic marker for Creutzfeldt-Jakob disease. Neurology. 2004; 63:443–449. [PubMed: 15304574]
3. Young GS, Geschwind MD, Fischbein NJ, et al. Diffusion-weighted and fluid-attenuated inversion recovery imaging in Creutzfeldt-Jakob disease: high sensitivity and specificity for diagnosis. AJNR Am J Neuroradiol. 2005; 26:1551–1562. [PubMed: 15956529]
4. Tschampa HJ, Kallenberg K, Kretzschmar HA, et al. Pattern of cortical changes in sporadic Creutzfeldt-Jakob disease. AJNR Am J Neuroradiol. 2007; 28:1114–1118. [PubMed: 17569970]
5. Zerr I, Kallenberg K, Summers DM, et al. Updated clinical diagnostic criteria for sporadic Creutzfeldt-Jakob disease. Brain. 2009; 132:2659–2668. [PubMed: 19773352]
6. Goldman S, Laird A, Flament-Durand J, et al. Positron emission tomography and histopathology in Creutzfeldt-Jakob disease. Neurology. 1993; 43:1828–1830. [PubMed: 8414042]
7. Grünwald F, Pohl C, Bender H, et al. 18F-fluorodeoxyglucose-PET and 99mTc-bicisate-SPECT in Creutzfeldt-Jakob disease. Ann Nucl Med. 1996; 10:131–134. [PubMed: 8814717]
8. Matochik JA, Molchan SE, Zametkin AJ, Warden DL, Sunderland T, Cohen RM. Regional cerebral glucose metabolism in autopsy-confirmed Creutzfeldt-Jakob disease. Acta Neurol Scand. 1995; 91:153–157. [PubMed: 7785428]
9. Holthoff VA, Sandmann J, Pawlik G, Schröder R, Heiss WD. Positron emission tomography in Creutzfeldt-Jakob disease. Arch Neurol. 1990; 47:1035–1038. [PubMed: 2204331]
10. Thomas A, Klein JC, Galldiks N, Hilker R, Grond M, Jacobs AH. Multitracer PET imaging in Heidenhain variant of Creutzfeldt-Jakob disease. J Neurol. 2006; 253:258–260. [PubMed: 16047109]
11. Clarençon F, Gutman F, Giannesini C, et al. MRI and FDG PET/CT findings in a case of probable Heidenhain variant Creutzfeldt-Jakob disease. J Neuroradiol. 2008; 35:240–243. [PubMed: 18466976]
12. Pichler R, Ciovica I, Rachinger J, Weiss S, Aichner FT. Multitracer study in Heidenhain variant of Creutzfeldt-Jakob disease: mismatch pattern of cerebral hypometabolism and perfusion imaging. Neuro Endocrinol Lett. 2008; 29:67–68. [PubMed: 18283251]
13. Tsuji Y, Kanamori H, Murakami G, et al. Heidenhain variant of Creutzfeldt-Jakob disease: diffusion-weighted MRI and PET characteristics. J Neuroimaging. 2004; 14:63–66. [PubMed: 14748211]
14. Friedland RP, Prusiner SB, Jagust WJ, Budinger TF, Davis RL. Bitemporal hypometabolism in Creutzfeldt-Jakob disease measured by positron emission tomography with [18F]-2-fluorodeoxyglucose. J Comput Assist Tomogr. 1984; 8:978–981. [PubMed: 6381559]
15. Henkel K, Zerr I, Hertel A, et al. Positron emission tomography with [(18)F]FDG in the diagnosis of Creutzfeldt-Jakob disease (CJD). J Neurol. 2002; 249:699–705. [PubMed: 12111302]
16. Engler H, Lundberg PO, Ekbom K, et al. Multitracer study with positron emission tomography in Creutzfeldt-Jakob disease. Eur J Nucl Med Mol Imaging. 2003; 30:85–95. [PubMed: 12483414]
17. Na DL, Suh CK, Choi SH, et al. Diffusion-weighted magnetic resonance imaging in probable Creutzfeldt-Jakob disease: a clinical-anatomic correlation. Arch Neurol. 1999; 56:951–957. [PubMed: 10448800]

18. World Health Organization. Emerging and Other Communicable Diseases, Surveillance and Control: Global Surveillance, Diagnosis and Therapy of Human Transmissible Spongiform Encephalopathies. Geneva: World Health Organization; 1998.
19. Geschwind MD, Josephs KA, Parisi JE, Keegan BM. A 54-year-old man with slowness of movement and confusion. Neurology. 2007; 69:1881–1887. [PubMed: 17984457]
20. Kropp S, Schulz-Schaeffer WJ, Finkenstaedt M, et al. The Heidenhain variant of Creutzfeldt-Jakob disease. Arch Neurol. 1999; 56:55–61. [PubMed: 9923761]
21. Manners DN, Parchi P, Tonon C, et al. Pathologic correlates of diffusion MRI changes in Creutzfeldt-Jakob disease. Neurology. 2009; 72:1425–1431. [PubMed: 19380702]
22. Geschwind MD, Potter CA, Sattavat M, et al. Correlating DWI MRI with pathologic and other features of Jakob-Creutzfeldt disease. Alzheimer Dis Assoc Disord. 2009; 23:82–87. [PubMed: 19266702]
23. Mittal S, Farmer P, Kalina P, Kingsley PB, Halperin J. Correlation of diffusion-weighted magnetic resonance imaging with neuropathology in Creutzfeldt-Jakob disease. Arch Neurol. 2002; 59:128–134. [PubMed: 11790240]
24. Urbach H, Klisch J, Wolf HK, Brechtelsbauer D, Gass S, Solymosi L. MRI in sporadic Creutzfeldt-Jakob disease: correlation with clinical and neuropathological data. Neuroradiology. 1998; 40:65–70. [PubMed: 9541914]
25. Kaneko M, Sugiyama N, Sasayama D, et al. Prion disease causes less severe lesions in human hippocampus than other parts of brain. Psychiatry Clin Neurosci. 2008; 62:264–270. [PubMed: 18588585]
26. Masullo C, Macchi G. Resistance of the hippocampus in Creutzfeldt-Jakob disease. Clin Neuropathol. 1997; 16:37–44. [PubMed: 9020394]
27. Hamaguchi T, Kitamoto T, Sato T, et al. Clinical diagnosis of MM2-type sporadic Creutzfeldt-Jakob disease. Neurology. 2005; 64:643–648. [PubMed: 15728285]
28. Jeong BH, Lee KH, Kim NH, et al. Association of sporadic Creutzfeldt-Jakob disease with homozygous genotypes at PRNP codons 129 and 219 in the Korean population. Neurogenetics. 2005; 6:229–232. [PubMed: 16217673]
29. Meissner B, Kallenberg K, Sanchez-Juan P, et al. MRI lesion profiles in sporadic Creutzfeldt-Jakob disease. Neurology. 2009; 72:1994–2001. [PubMed: 19506221]
30. Bavis J, Reynolds P, Tegeler C, Clark P. Asymmetric neuroimaging in Creutzfeldt- Jakob disease: a ruse. J Neuroimaging. 2003; 13:376–379. [PubMed: 14569834]
31. Cambier DM, Kantarci K, Worrell GA, Westmoreland BF, Aksamit AJ. Lateralized and focal clinical, EEG, and FLAIR MRI abnormalities in Creutzfeldt-Jakob disease. Clin Neurophysiol. 2003; 114:1724–1728. [PubMed: 12948802]
32. Mandell AM, Alexander MP, Carpenter S. Creutzfeldt-Jakob disease presenting as isolated aphasia. Neurology. 1989; 39:55–58. [PubMed: 2642613]
33. Kirk A, Ang LC. Unilateral Creutzfeldt-Jakob disease presenting as rapidly progressive aphasia. Can J Neurol Sci. 1994; 21:350–352. [PubMed: 7874620]
34. Yamanouchi H, Budka H, Vass K. Unilateral Creutzfeldt-Jakob disease. Neurology. 1986; 36:1517–1520. [PubMed: 3531919]
35. Zhang WJ, Westover MB, Keary CJ. Premortem diagnosis of sporadic Creutzfeldt- Jakob disease aided by positron-emission tomography imaging. AJNR Am J Neuroradiol. 2011; 32:E18. [PubMed: 21071534]
36. Prasad S, Lee EB, Woo JH, Alavi A, Galetta SL. Photo essay. MRI and positron emission tomography findings in Heidenhain variant Creutzfeldt-Jakob disease. J Neuroophthalmol. 2010; 30:260–262. [PubMed: 20581692]

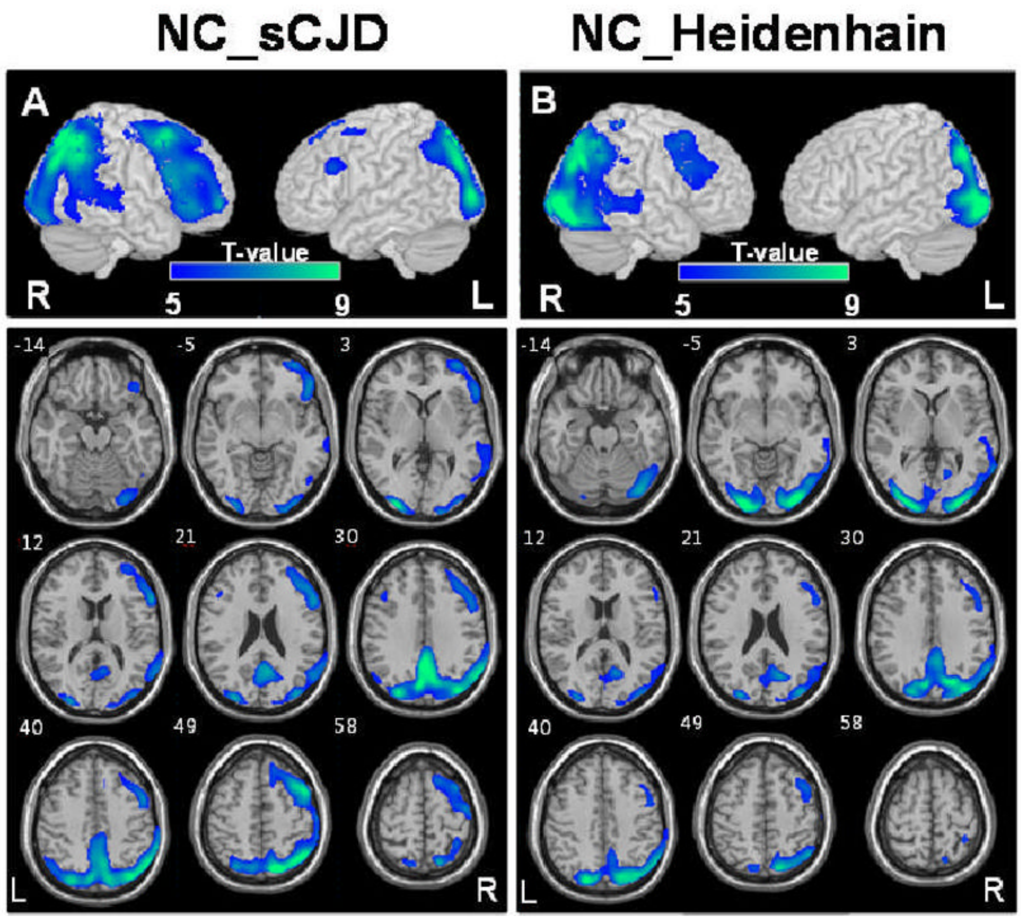

Figure 1.

Areas with significant glucose hypometabolism in sCJD (A) and the Heidenhain variant of sCJD (B) compared with controls are superimposed on surface rendered and transaxial images, respectively, at the threshold of $p < 0.05$, corrected for multiple comparison, k = 100. The numbers in the axial images indicate the distance (mm) from the anterior-posterior commissure plane. NC = normal controls, R = right, L = left.

Table 1

Patient demographics

Patient No.	Sex	Onset age (y)	Interval to PET (mon)	First symptoms	Clinical sign/symptom	EEG	14-3-3 protein	Codon 129 in PRNP	Regions with high signal intensities on DWI MRI	WHO CJD Diagnosis**
1	M	63	2.8	Gait disturbance	Gait ataxia, dysarthria, myoclonus, insomnia, visual hallucination, macropsia, dementia	PSWC	NP	NP	RF, LF, RP, RT, RO, LO, RB	Probable
2*	F	69	2.1	Visual disturbance	Visual hallucination, blurred vision, abulia, pyramidal sign, myoclonus parkinsonism, dementia	GCS	NP	NP	RF, LF, RP, LP, RT, LT, RO, LO, RB, LB	Possible
3*	M	54	4.7	Visual disturbance	Metamorphopsia, dyschromatopsia, gait ataxia, dysarthria, parkinsonism, psychiatric symptoms, insomnia, dizziness, dementia	GCS	NP	NP	RF, RP, LP, RT, RO, RB, LB	Possible
4	M	66	1.4	Obtundation	Gait ataxia, dysarthria, dizziness, dysphagia, dementia	PSWC	NP	NP	RF, LF, RT, RO, LO, RB, LB	Probable
5	F	61	3.8	Dysarthria	Aphasia, abulia, gait ataxia, myoclonus, pyramidal sign, parkinsonism, sensory symptoms, dizziness, metamorphopsia, dyschromatopsia, dementia	PSWC	NP	NP	RF, LF, RP, LP, RT, LT, RO, LO, RB, LB, LTh	Probable
6*	M	36	8.0	Visual disturbance	Micropsia, metamorphosia, diplopia, blurred vision, visual hallucination, tremor, auditory hallucination, gait ataxia, dysarthria, myoclonus, parkinsonism, dementia	GCS	NP	MM	RF, RP, LP, RT, LT, RO, LO, RB, LB	Definite
7	M	62	2.0	Memory impairment	Aphasia, gait ataxia, parkinsonism, myoclonus, dementia	GCS	Positive	MM	RF, LF, LT	Probable
8*	F	62	4.8	Visual disturbance	Macropsia, dyschromatopsia, metamorphopsia, diplopia, dizziness, dysarthria, myoclonus, dementia	PSWC	Positive	MM	LP, LT, LO	Probable
9	F	75	0.4	Dysarthria	Confusion, gait ataxia, pyramidal sign, dementia	Normal	Negative	MM	RF, LF, RB	Possible
10*	F	68	1.2	Visual disturbance	Blurred vision, abulia, gait ataxia, myoclonus, psychiatric symptoms, dementia	PSWC	NP	NP	RF, LF, RP, LP, RT, RO, LO, RB	Probable

Patient No.	Sex	Onset age (y)	Interval to PET (mon)	First symptoms	Clinical sign/symptom	EEG	14-3-3 protein	Codon 129 in PRNP	Regions with high signal intensities on DWI MRI	WHO CJD Diagnosis**
11	F	60	0.7	Tremor	Tremor, aphasia, abulia, dysarthria, dementia	GIS	Positive	MM	RF, LF, RP, LP, RT, LT, LB, RC, LC	Probable

No = number; y = years; mon = months; PET = positron emission tomography; EEG = electroencephalogram; PRNP = prion protein gene; PSWC = periodic sharp and wave complexes; GC S = generalized continuous slow waves; GIS = generalized intermittent slow waves; NP = not performed; MM = methionine homozygosity at codon 129 in PRNP; * = Heidenhain variant; RF = right frontal cortex; LF = left frontal cortex; RP = right parietal cortex; LP = left parietal cortex; RT = right temporal cortex; LT = left temporal cortex; RO = right occipital cortex; LO = left occipital cortex; RB = right basal ganglia; LB = left basal ganglia; LTh = left thalamus; RC = right cerebellum; LC = left cerebellum ** All subjects met UCSF probable sCJD diagnostic criteria, which allow the use of MRI in place of the EEG or 14-3-3.